Synthesis of Magnetic Nanoparticles of Fe_3O_4 and $CoFe_2O_4$ and Their Surface Modification by Surfactant Adsorption

Shi-Yong Zhao,[†] Don Keun Lee, Chang Woo Kim, Hyun Gil Cha, Young Hwan Kim, and Young Soo Kang[*]

Department of Chemistry, Pukyong National University, Busan 608-737, Korea. [*]E-mail: yskang@dophin.pknu.ac.kr
Received July 28, 2005

Fe_3O_4 and $CoFe_2O_4$ magnetic nanoparticles have been synthesized successfully in aqueous solution and coated with oleic acid. The solid and organic solution of the synthesized nanoparticles was obtained. Self-assembled monolayer films were formed using organic solution of these nanoparticles. The crystal sizes determined by Debye-Scherre equation with XRD data were found close to the particle sizes calculated from TEM images, and this indicates that the synthesized particles are nanocrystalline. Especially, EDS, ED, FT-IR, TGA/DTA and DSC were used to characterize the nanoparticles and the oleic acid adsorption, and it was found that oleic acid molecule on the Fe_3O_4 nanoparticle is a bilayer adsorption, while that on $CoFe_2O_4$ nanoparticle is single layer adsorption. The superparamagnetic behavior of the nanoparticles was documented by the hysteresis loop measured at 300 K.

Key Words : Magnetic nanoparticles, Surfactant adsorption, Fe_3O_4, $CoFe_2O_4$

Introduction

As holding many novel physical and chemical properties than other nanoparticles, magnetic nanoparticles have been paid much attention.[1-7] One of the scientific interests is the magnetic properties of single-domain magnetic nanoparticle assemblies, and the technological interest is that the magnetic nanoparticles would find wide applications.[8-12]

There exist several problems about the investigation of magnetic nanoparticles, and these exist in other nanoparticles as well. The first is how to obtain monodispersed nanoparticle and their composite. The second is how to assemble the nanoparticles into ordered one-dimensional, two-dimensional, or three-dimensional spatial configurations, and many techniques have been used to prepare ordered structure of nanoparticles, including LB technique,[13] self-assembly technique,[14] electrophoretic deposition[15] and magnetophoretic deposition.[16] The third is the characterization of the nanoparticles and their assembly, and usually UV-vis, FT-IR, XRD, TGA/DAT, zeta potential, XPS, TEM, SEM, AFM, STM were used. Especially, the magnetic properties of magnetic nanoparticles and their assembly were characterized by Mössbauer spectra, magnetization curve, ferromagnetic resonance (FMR),[17] magnetoresistance (R(H)), and EPR.[18] The forth is the applications of the nanoparticles and their assembly in various fields.

The syntheses of uniform-sized magnetic metal nanoparticles have been reported.[19-22] Nevertheless, little work on the fabrication of monodispersed and crystalline Fe_3O_4 and $CoFe_2O_4$ nanoparticles has been found. In this paper, highly crystalline and monodispersed Fe_3O_4 and $CoFe_2O_4$ magnetic crystalline nanoparticles were obtained using chemical coprecipitation in aqueous solution. Two kinds of nanoparticles were characterized by XRD, TEM, EDS, ED, FT-IR, TGA/DTA, DSC and VSM and their properties were compared. It was found that oleic acid molecule on the Fe_3O_4 nanoparticle is a bilayer adsorption, while that on $CoFe_2O_4$ nanoparticle is single layer adsorption.

Experimental Section

Preparation of Fe_3O_4 nanoparticle by chemical coprecipitation in aqueous solution. All the chemicals, including $FeCl_2 \cdot 4H_2O$(99+%), $FeCl_3 \cdot 6H_2O$ (99+%), sodium oleate (98%), $CHCl_3$ (HPLC grade) and CH_3COCH_3 (HPLC grade), were obtained from Aldrich Chemical Co. and used without further purification. Distilled water was passed through a six-cartridge Barnstead Nanopure II purification train consisting of Macropure pretreatment and deoxygenated by bubbling with N_2 gas for 1 h prior to the use, and the main synthetic steps were carried out under a N_2 gas atmosphere. Typically,[1] 2.70 g of $FeCl_3 \cdot 6H_2O$ and 1.00 g of $FeCl_2 \cdot 4H_2O$ were dissolved into 50 mL of water. To this solution, 25 mL of 25% ammonia was added at 80 °C under vigorous stirring. The stirring was continued for 30 min and the reacted mixture was cooled to room temperature. The precipitate was isolated in a magnetic field and washed with 20 mL of water. The precipitate was redispersed in 20 mL of water, 1 g of sodium oleate in 10 mL of water was added, and stirring for 1 h at room temperature. Then the suspension was slowly acidified with 1 M HCl until the pH = 4-5 and an oily black precipitate appeared. The precipitate was dissolved into 230 mL of chloroform, obtained a transparent solution. In order to remove the larger particle, 20 mL of acetone was added to the chloroform solution, and the solution became cloudy. Laying for 1 h, the larger particle sedimentated to the bottom and the solution became transparent again. The transparent solution was removed to another beaker and 230 mL of acetone was added to

[†]Permanent address: Department of Chemistry, Shandong University, Jinan, 250100, P.R. China

precipitate most of the particle, only the smaller particle existed still in the solution. The precipitate was dried in air naturally and could be soluble in chloroform readily.

Preparation of $CoFe_2O_4$ nanoparticle in aqueous solution. A 10 mL water, dissolving 0.54 g $FeCl_3 6H_2O$ and 0.238 g $CoCl_2 \cdot 6H_2O$, resulted in an aqueous solution. Dissolving 1.2 g NaOH in 10 mL water. Adding NaOH solution into the prepared solution under stirring at 80 °C. The stirring was continued for 30 min and cooled to room temperature and the precipitate was isolated in a magnetic field, and washed wish water three times. Coating was carried out by adding aqueous solution of 0.2 g sodium oleate in 10 mL water and stirring for 1 h. The suspension was slowly acidified with 1 M HCl until the pH = 5, and an oily black precipitate appeared. The oily black precipitate was soluble in chloroform. The removal of bigger and smaller particles was carried out as the same procedure for Fe_3O_4 nanoparticle.

Characterization of nanoparticles by XRD, TEM, EDS, ED, FT-IR, TGA-DTA, DSC and VSM. The structural properties of synthesized nanoparticles were analyzed by X-ray powder diffraction (XRD) with a Philips X'Pert-MPD System. The average diameter of the crystals was estimated using Scherrer's formula. TEM experiments and corresponding electron diffraction (ED) were carried out on a JEOL JEM2010 transmission electron microscope operated at 200 kV, and EDS was performed with an EDAX X-ray energy-dispersive analysis system attached to the JEOL JEM2010 transmission electron microscope. TEM samples were prepared on the 400 mesh copper grid coated with carbon. A drop of the nanoparticle solution was carefully placed on the grid and dried in air. The size distributions of the particles were measured from enlarged photographs of the TEM images. The transmission FT-IR spectra were recorded with a Perkin Elmer Spectrum 2000. Thermogravimetric analysis (TGA) and differential thermal analysis (DTA) studies were carried out using a Perkin Elmer (USA) TGA7 Therogravimetric Analyzer at a rate of 10 °C/min in a N_2 atmosphere. Differential scanning calorimetry (DSC) measurements were performed using a Perkin Elmer differential scanning calorimeter pyris 1 at a ramp rate of 10 °C/min in a N_2 atmosphere. The magnetization curves were characterized with Lake Shore 7300 VSM.

Results and Discussion

Generally, XRD can be used to characterize the crystallinity of nanoparticle, and it gives an average diameters of all the nanoparticles. The XRD patterns of the Fe_3O_4 and $CoFe_2O_4$ nanoparticle samples are shown in Figure 1. The discernible peaks in Figure 1(a) can be indexed to (220), (311), (400), (333), and (440) planes of a cubic unit cell, which corresponds to that of magnetite structure (JCPDS card no. 79-0418), and the discernible peaks in Figure 1(b) can be indexed to (220), (311), (400), (511), and (440) planes of a cubic unit cell, which corresponds to cubic spinel structure of cobalt iron oxide (JCPDS card, no. 22-1086).

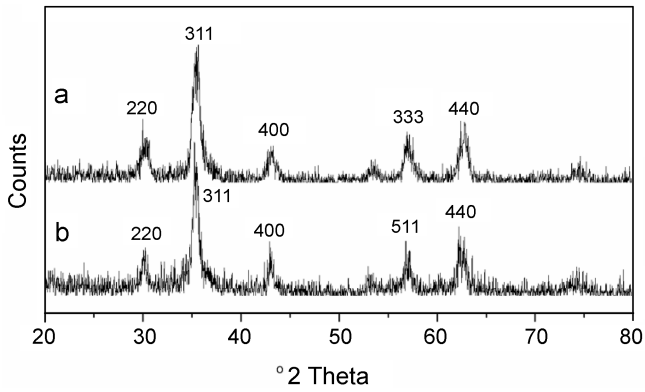

Figure 1. XRD patterns of (a) Fe_3O_4 and (b) $CoFe_2O_4$ nanoparticles.

The mean crystal sizes determined by Debye-Scherre equation with XRD data have been found 8.8 nm for Fe_3O_4 and 14.8 nm for $CoFe_2O_4$, which are close to the particle sizes calculated from TEM images (9.1 nm for Fe_3O_4 and 14.6 nm for $CoFe_2O_4$). This indicates that both of the Fe_3O_4 and $CoFe_2O_4$ are all nanocrystalline. Figure 2(a) is the TEM of Fe_3O_4 nanoparticle monolayer formed by self-assembly when a drop of the nanoparticle chloroform solution was carefully placed on the grid and dried in air. Most of the Fe_3O_4 particles are irregular spherical. A monolayer of nanoparticle is observed from the image with almost no any multiayer on it. The area of single self-assembled monolayer was calculated of about 50 μm^2 from the TEM with lower magnification. Insertion in Figure 2(a) is the histogram of the size distribution of Fe_3O_4 nanoparticles obtained from enlarged image of Figure 2(a). The mean size of Fe_3O_4 nanoparticles is 9.1 nm with a standard deviation 2.3 nm. Figure 2(b) is the TEM image of $CoFe_2O_4$ nanoparticle monolayer formed by self-assembly. Most of the $CoFe_2O_4$ particles are also irregular spherical. The area of single self-assembled monolayer was filled the whole mesh of the copper grid observed from the TEM with lower magnification. The histogram of the size distribution of $CoFe_2O_4$ nanoparticles obtained from enlarged image of Figure 2(b) is shown in the insertion in Figure 2(b). The mean size is 14.6 nm and the standard deviation is 2.8 nm. EDS results support the formation of nanoparticles. Figure 3(a) shows the EDS of the Fe_3O_4 nanoparticles, the particles contain Fe element and Figure 3(b) shows the EDS of the $CoFe_2O_4$ nanoparticles, the particles contain two elements of Fe and Co. The peaks attributed to Cu were caused by copper grid. Electron diffraction (ED) was also used to check the structure of the nanoparticle. In Figure 4(a) it revealed densed ring patterns with d spacings of 3.02, 2.55, 2.11, 1.64, 1.51 Å, which match the standard body centered cubic spinel structure of magnetite lines (JCPDS card, no. 79-0418). In Figure 4(b) it revealed dense ring patterns with d spacings of 3.01, 2.54, 2.11, 1.63, 1.49 Å, which match the standard body centered cubic spinel structure of cobalt iron oxide lines (JCPDS card, no. 22-1086). These results are agreeable to the XRD results. Figure 5(b) is FT-IR spectrum

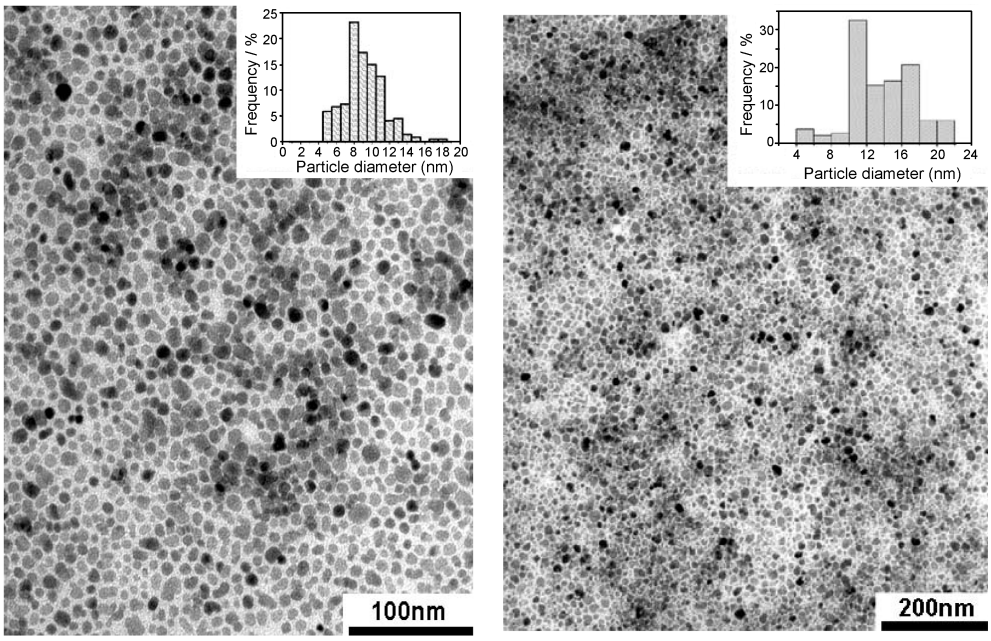

Figure 2. TEM images of (a) Fe_3O_4 and (b) $CoFe_2O_4$ nanoparticles.

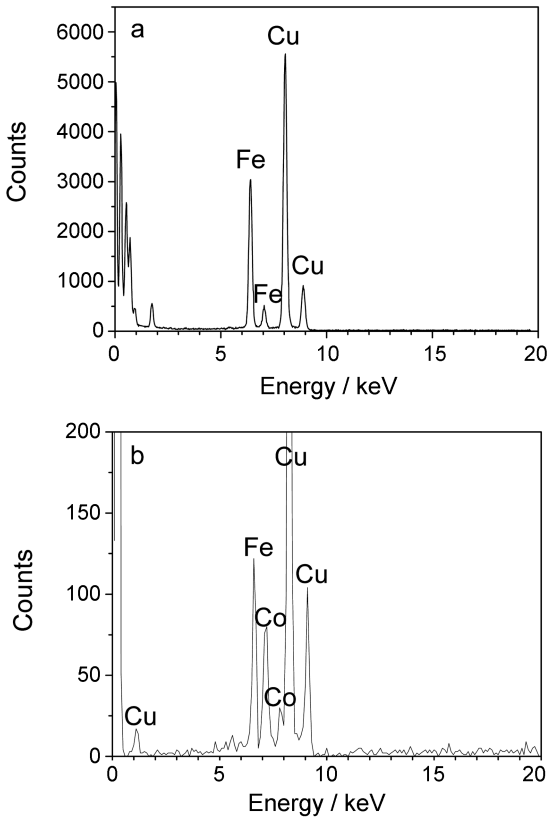

Figure 3. EDS patterns of (a) Fe_3O_4 and (b) Co Fe_2O_4 nanoparticles.

of pure oleic acid. Oleic acid shows a strong absorption peak of carbonyl stretch band around 1706 cm^{-1}.

The strong bands at 2857 and 2923 cm^{-1} belong to methylene and methyl symmetric stretching vibration, respectively. Figure 5(a) is FT-IR spectrum of Fe_3O_4 nanoparticle coated with oleic acid. The peak around 1706 cm^{-1} still exists, meaning that some free oleic acid in the Fe_3O_4 nanoparticle sample, as will be supported by the TGA/DTA results below. A strong peak around 1539 cm^{-1} appears, which is interpreted as the complexation between the carboxylate and Fe_3O_4 nanoparticles was formed. However, the peak around 1706 cm^{-1} disappears completely and a strong peak around 1559 cm^{-1} was shown in FT-IR spectrum of $CoFe_2O_4$ nanoparticle coated with oleic acid as shown in Figure 5(c). This indicates that there is no free oleic acid in the $CoFe_2O_4$ nanoparticle sample and the complexation between the carboxylate and $CoFe_2O_4$ nanoparticles was formed, this will be supported by the TGA/DTA results below. Figure 6(a) shows the TGA/DTA curves of Fe_3O_4 nanoparticle coated with oleic acid. There are five derivative peaks in the DTA curve which corresponding to the five mass losses in the TGA curve. The first peak is at about 118 °C, and the percentage mass loss is about 0.80%, which probably due to the removal of surface adsorbed organic solvent and surface hydroxyls. The second peak is at about 253 °C, which is approximately the boiling or decomposition temperature of oleic acid (b.p., 94-195 °C/1.2 mmHg), and the percentage of mass loss is about 3.9%, which probably due to the removal of free oleic acid on the Fe_3O_4 nanoparticles. The position of third peak is at about 377 °C, and the percentage of mass loss is about 6.6%, which corresponds to the oleic acid molecules that bind directly with Fe_3O_4 nanoparticle. The mass loss, as well as the high adsorption temperature, confirms strong binding between the oleic acid molecules and Fe_3O_4 nanoparticle. The bilayer adsorption of oleic acid molecules is agreeable to the results of Markovich *et al.*[23] The compelling evidence for bilayer formation in fatty acid coated magnetite particles was provided by Hatton et al using TGA, DSC [24] and small-

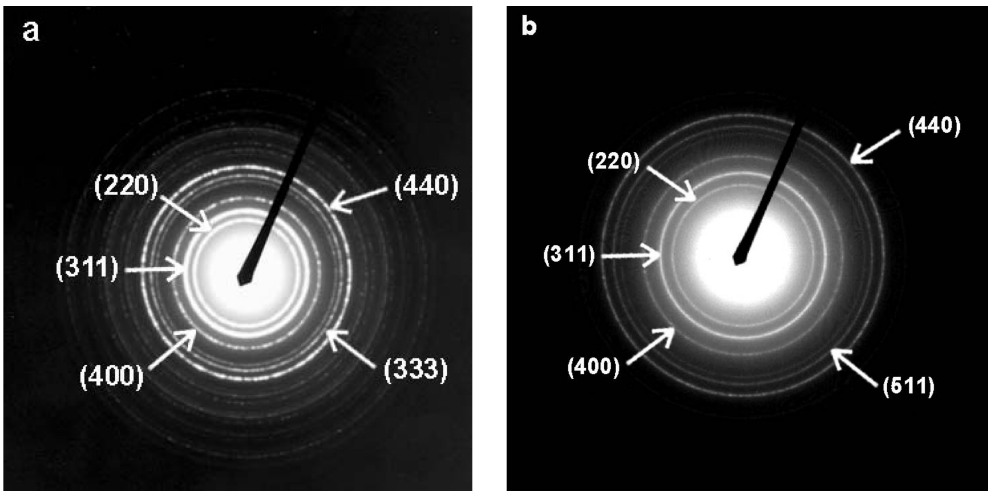

Figure 4. ED patterns of (a) Fe_3O_4 and (b) Co Fe_2O_4 nanoparticles.

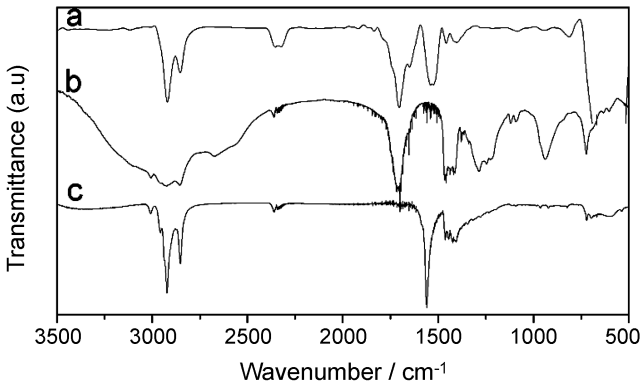

Figure 5. FT-IR spectra of (a) Fe_3O_4 nanoparticle coated with oleic acid, (b) pure oleic acid and (c) $CoFe_2O_4$ nanoparticle coated with oleic acid.

angle neutron scattering (SANS).[25] The temperature of fourth peak is as high as 712 °C, and the percentage of mass loss is about 5.8%, which is due to the phase transition from Fe_3O_4 to FeO, because FeO is thermodynamically stable above 570 °C in phase diagram of the Fe-O system.[26] At 752 °C, there still exist a derivative peak corresponding to a percentage mass loss of 4.4%, this maybe the deoxidation of FeO since the TGA/DTA analysis was carried out under the N_2 atmosphere. There are also five derivative peaks in the DTA curve of $CoFe_2O_4$ nanoparticle coated with oleic acid which corresponds to the five mass losses in the TGA curve as shown in Figure 6(b). The peak temperatures are 100 °C, 257 °C, 376 °C, 620 °C, 681 °C and the corresponding percentages of mass losses are about 1.2%, 2.2%, 15.4%, 6.3%, 5.4%, respectively. Comparing with the TGA/DTA curves of Fe_3O_4 nanoparticles, there exist two obvious differences. First, the second peak corresponding to the removal of free oleic acid is very lower, this means that there is few free oleic acid molecules in $CoFe_2O_4$ nanoparticle sample, which is agreeable to FTIR results above. Secondly, the monument of oleic acid molecules binding directly with $CoFe_2O_4$ nanoparticle is as high as 15.4% (the third peak), which is even higher than the sum of free oleic acid and

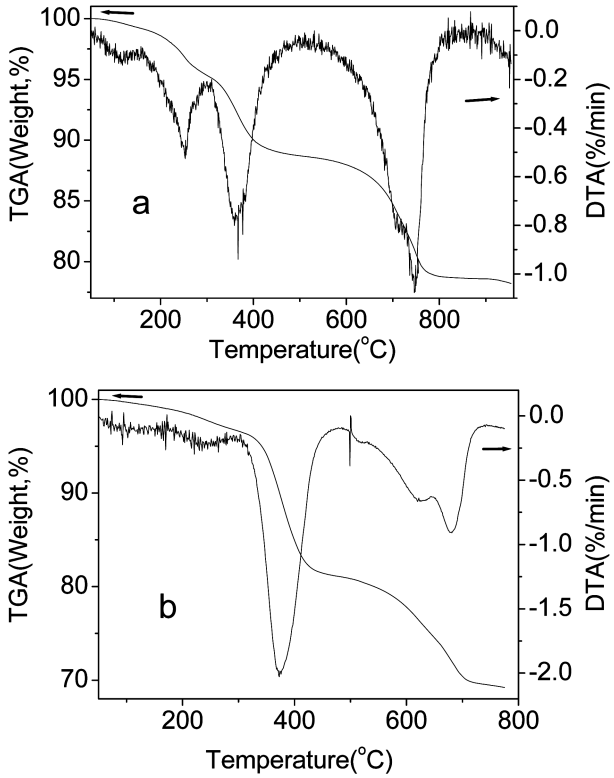

Figure 6. TGA/DTA curves of (a) Fe_3O_4 and (b) $CoFe_2O_4$ nanoparticles coated with oleic acid.

binding directly oleic acid of Fe_3O_4 nanoparticle sample (3.9% + 6.6%). The coverage of the oleic acid molecules binding directly with Fe_3O_4 and $CoFe_2O_4$ nanoparticles can be calculated from the TGA results and assumed that all the nanoparticles were spheres with the diameter of 9.1 nm for Fe_3O_4 nanoparticle and 14.6 nm for $CoFe_2O_4$ nanoparticle. The coverage was 0.80 nm^2/molecule for Fe_3O_4 nanoparticle and 0.19 nm^2/molecule for $CoFe_2O_4$ nanoparticle. Owing to the fact that in close-packed oleic acid layer each molecule occupies an area of 0.21 nm^2, it can be concluded that in the case of $CoFe_2O_4$ nanoparticle the oleic acid molecules

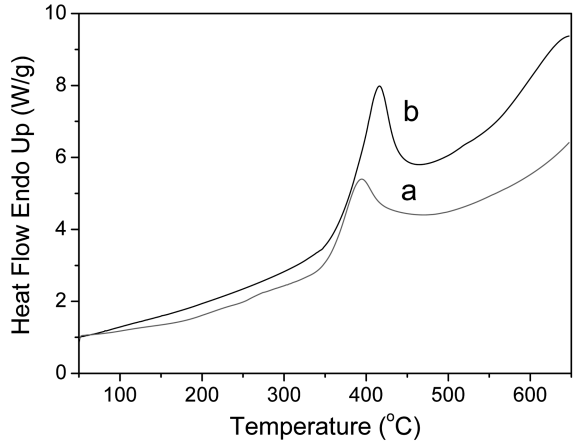

Figure 7. DSC curves of (a) Fe_3O_4 and (b) $CoFe_2O_4$ nanoparticles coated with oleic acid.

binding directly with nanoparticle were close-packed and even crowded, maybe a few molecules were a little far from the surface of nanoparticle and were sandwiched between two molecules that contact with the surface of nanoparticle directly. Because the high curvature of the nanoparticle surface would lead to greater space between the two molecules far from the surface of nanoparticle. The higher monument of oleic acid results in the better solubility of $CoFe_2O_4$ nanoparticle sample in organic solvent than Fe_3O_4 nanoparticle sample. Figure 7 shows the DSC curves of the Fe_3O_4 and $CoFe_2O_4$ nanoparticles coated with oleic acid. A large endothermic transition was found from 45 °C to 650 °C. The transition is at 395 °C for Fe_3O_4 nanoparticles, and 416 °C for $CoFe_2O_4$ nanoparticles, which is related to the oleic acid molecules binding directly with nanoparticle. The higher peak temperature and larger enthalpy for $CoFe_2O_4$ nanoparticles than those for Fe_3O_4 nanoparticles mean that the monument of oleic acid molecules binding directly with $CoFe_2O_4$ nanoparticle are larger than that with Fe_3O_4 nanoparticle, and this has been confirmed by the TGA/DTA results.

Hatton *et al.*[24] thought that in the bilayer surfactant stabilized Fe_3O_4 nanoparticle system, there exit partial interpenetration of the hydrocarbon tails of the primary and secondary surfactants. This is agreeable to the case of our Fe_3O_4 nanoparticle coating with bilayer adsorption of oleic acid molecules. But for the case of our $CoFe_2O_4$ nanoparticle, the coverage of the primary oleic acid molecules is so high that the steric constraints of the hydrocarbon chains preclude the formation of hydrocarbon tails interpenetration of the primary and secondary oleic acid layer, because there is no enough space between the hydrocarbon tails of the primary layer. So the amount of oleic acid in secondary layer is very little.

The superparamagnetic behavior is documented by the hysteresis loop measured at 300 K as shown in Figure 8. There is almost immeasurable coercivity (0.814 Oe) for Fe_3O_4 at room temperature, this indicates that the Fe_3O_4 particle are superparamagnetic and nanosized. The saturation magnetization, M_s, are 60.1 emu/g for Fe_3O_4, which are lower than that of bulk magnetite particles (M_{bulk} = 92 emu/g). The decrease in M_s is due to superparamagnetism of magnetite particles, which occur when the particle size decreases below 30 or 20 nm.[27,28] From the magnetization curves it can be seen that the magnetization does not saturate for Fe_3O_4, even at 10000 Oe. This phenomenon can be explained from the shape and size distributions observed by TEM. Comparing with Fe_3O_4 nanoparticle, $CoFe_2O_4$ nanoparticle has larger coercivity (243 Oe) at room temperature. This means that $CoFe_2O_4$ nanoparticle is a not very hard magnetic material.

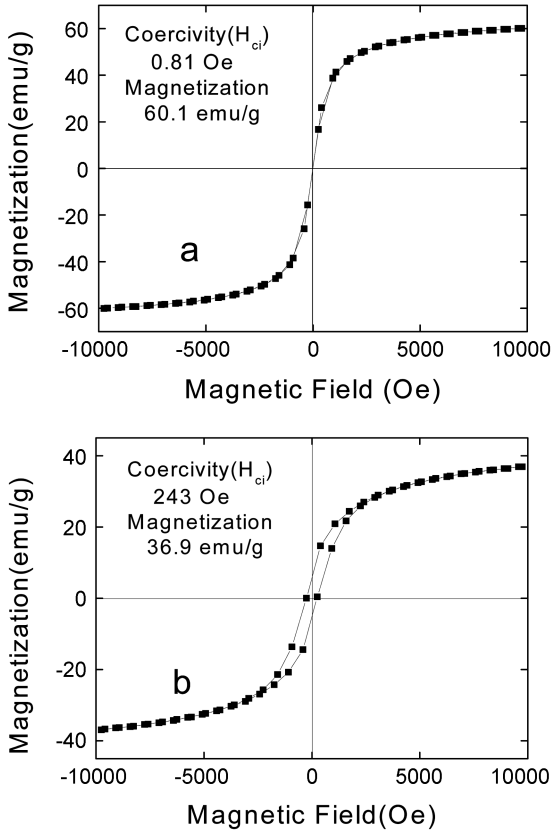

Figure 8. Magnetization curve versus applied field at 300 K for (a) Fe_3O_4 and (b) $CoFe_2O_4$ nanoparticles coated with oleic acid.

Conclusions

Fe_3O_4 and $CoFe_2O_4$ nanoparticle has been synthesized successfully by chemical coprecipitation methods in aqueous solution and coated with oleic acid. These nanoparticles can be transferred to organic solution and the self-assembled monolayer films of these nanoparticles were formed using the organic solution. Both of the two nanoparticles are spherical and the particles are magnetite structure and monocrystalline. FT-IR, TGA/DTA, DSC results indicate that the oleic acid molecules on the surface of Fe_3O_4 nanoparticle is a bilayer adsorption, while that on $CoFe_2O_4$ nanoparticle maybe a single layer adsorption. The superparamagnetic behavior was documented by the hysteresis

loop measured at 300 K, and it was found that Fe_3O_4 nanoparticle has good superparamagnetic and $CoFe_2O_4$ nanoparticle is a not very hard magnetic material.

Acknowledgment. This research is financially supported by National Research Laboratory Program of Korean Ministry of Science and Technology.

References

1. Sun, S.; Anders, S.; Hamann, H. F.; Thiele, J.-U.; Baglin, J. E. E.; Thomson, T.; Fullerton, E. E.; Murray, C. B.; Terris, B. D. *J. Am. Chem. Soc.* **2002**, *124*, 2884.
2. Fried, T.; Shemer, G.; Markovich, G. *Adv. Mater.* **2001**, *13*, 1158.
3. Ahmed, S. R.; Kofinas, P. *Macromolecules* **2002**, *35*, 3338.
4. Albuquerque, A. S.; Ardisson, J. D.; Macedo, W. A. A.; Lopez, J. L.; Paniago, R.; Persiano, A. I. C. *J. Magn. Magn. Mater.* **2001**, *226-230*, 1379.
5. Gonzalez-Carreno, T.; Morales, M. P.; Serna, C. J. *Materials Letters* **2000**, *43*, 97.
6. Kim, K. *Bull. Korean Chem. Soc.* **1987**, *8*, 430.
7. Chi, E. O.; Kang, J. K.; Kwon, Y. U.; Hur, N. H. *Bull. Korean Chem. Soc.* **1997**, *18*, 1238.
8. Sun, S.; Murray, C. B.; Weller, D.; Folks, L.; Moser, A. *Science* **2000**, *278*, 1989.
9. Rosensweig, R. *Ferrohydrodynamics*; Cambridge University Press: Cambridge, 1985.
10. Kim, D. K.; Zhang, Y.; Kehr, J.; Klason, T.; Bjelke, B.; Muhammed, M. *J. Magn. Magn. Mater.* **2001**, *225*, 256.
11. Roger, J.; Pons, J. N.; Massart, R.; Halbreich, A.; Bacri, J. C. *Euro. Phys.: Appl. Phys.* **1999**, *5*, 321.
12. Kang, E. A.; Park, J. N.; Hwang, Y. S.; Kang, M. S.; Park, J. G.; Hyeon, T. H. *J. Phys. Chem. B* **2004**, *108*, 13932.
13. Meldrum, F. C.; Kotov, N. A.; Fendler, J. H. *Langmuir* **1994**, *10*, 2035.
14. Motte, L.; Billoudet, F.; Pileni, M. P. *J. Phys. Chem.* **1995**, *99*, 16425.
15. Giersig, M.; Mulvaney, P. *J. Phys. Chem.* **1993**, *97*, 6334.
16. Giersig, M.; Hiigendorff, M. *J. Phys. D: Appl. Phys.* **1999**, *32*, L111.
17. Bizdoaca, E. L.; Spasova, M.; Farle, M.; Hilgendorff, M.; Caruso, F. *J. Magn. Magn. Mater.* **2002**, *240*, 44.
18. Cannas, C.; Gatteschi, D.; Musinu, A.; Piccaluga, G.; Sangregorio, C. *J. Phys. Chem. B* **1998**, *102*, 7721.
19. Park, S.-J.; Kim, S.; Lee, S.; Khim, Z. G.; Char, K.; Hyeon, T. *J. Am. Chem. Soc.* **2000**, *122*, 8581.
20. Puntes, A. F.; Krishnan, K. M.; Alivisatos, A. P. *Science* **2001**, *291*, 2115.
21. Sun, S.; Murray, C. B. *J. Appl. Phys.* **1999**, *85*, 4325.
22. Suslick, K. S.; Fang, M.; Hyeon, T. *J. Am. Chem. Soc.* **1996**, *118*, 11960.
23. Sahoo, Y.; Pizem, H.; Fried, T.; Golodnitsky, D.; Burstein, L.; Sukenik, C. N.; Markovich, G. *Langmuir* **2001**, *17*, 7907.
24. Shen, L.; Laibinis, P. E.; Hatton, T. A. *Langmuir* **1999**, *15*, 447.
25. Shen, L.; Stachowiak, A.; Fateen, S.-E. K.; Laibinis, P. E.; Hatton, T. A. *Langmuir* **2001**, *17*, 288.
26. Darken, L. S.; Gurry, R. W. *J. Am. Chem. Soc.* **1946**, *68*, 798.
27. Han, D. H.; Wang, J. P.; Luo, H. L. *J. Magn. Magn. Mater.* **1994**, *136*, 176.
28. Lee, L.; Isobe, T.; Senna, M. *J. Colloid. Interface. Sci.* **1996**, *177*, 490.